Offshore floating wind farms cost reduction assessment

Jakub Grzegorz Strąg
jakub.strag@gmail.com

Instituto Superior Ténico, Universidade de Lisboa, Portugal

December 2022

Abstract

The need for a faster energy transition towards a carbon-neutral society has accelerated the support and development of offshore floating wind technologies. However, the necessity for cost reductions to make offshore energy projects viable and more attractive to developers require further research on new strategies for wind farm cost reductions and performance enhancements. The main objective of this work is to evaluate techno-economically some of these strategies. The goals of this work were achieved through aero-hydro-servo-elastic numerical simulations and cost-modelling of twenty-five different wind farm case studies, considering variations in turbine spacing distances, turbine hub heights, farm layouts and the floating platform size. The main farm evaluation factors addressed in this work are the annual electricity production, farm energy losses due to the wake effects, farm capacity factor, the levelized cost of energy (LCOE) and an energy yield density factor that is introduced in this thesis. Based on this study, it can be noticed that turbine hub height variations do not necessarily show promising LCOE reductions due to lower wind resources and insignificant cost reductions. The platform size reduction was estimated to have a low impact on the wind farm LCOE. Different wind farm layouts, on the other hand, can significantly decrease the wake losses and the LCOE by up to 17.2%. This study provides a good base for further techno-economic analysis of different wind farm configurations, including the wind turbine row spacing, turbine hub heights and wind farm layouts. It also presents recommendations for cost-reduction analysis tools and methodologies.

Keywords: Offshore wind energy, floating offshore wind turbines, LCOE, techno-economic assessment, cost reductions, wake effects

1. Introduction

Since the 19th century, global greenhouse gas (GHG) emissions have been rising, reaching the highest peak in 2019. Fossil fuels had the highest contribution to GHG emission levels, reaching 36.71 billion tons in 2019. The largest share of these emissions (34%) was produced by the energy sector for electricity generation purposes [1].

Increasing concerns about rising GHG emissions and climate change consequences led to the establishment of the international Paris Agreement in 2015 or the United Nations' 17 Sustainable Development Goals (SDGs) along with The 2030 Agenda for Sustainable Development, which discuss the importance of the GHG emmisions' reduction.

Considering the above-presented concerns, it is important to continue renewable energy solutions' development and technological sophistication. Out of the available renewable energy sources, wind energy is estimated to have the highest CO_2 reduction capability by the year 2050 [2]. Furthermore, due to increasing onshore wind limitations [3], offshore wind energy is getting more recognition, providing better exploitation of wind resources, the possibility of larger turbine utilization and lower environmental impacts [3]. Among the offshore wind energy solutions, floating offshore wind (FOW) farms are showing promising outcomes, thanks to, for example, the onshore manufacturing and assembly or the deep water conditions utilization [3]. However, the levelized cost of energy (LCOE) of floating offshore wind projects is still high compared to other solutions [3].

One of the main factors contributing to the LCOE reduction is the increase in the production of electricity by reducing the overall farm energy losses [4]. One way of the energy losses reduction in FOW is the reduction of the wake effect on the subsequent turbines, which can be done by increasing the spacing between the turbines [5], different geometrical layouts of the turbines in a farm [5], or the differentiation in the subsequent turbine hub heights [6].

The research done by [5] shows that different shapes of wind farms can have an impact on total electricity generation and wind farm wake losses.

Non-orthogonal wind farm layouts may decrease the wake losses and increase the energy yield from a farm.

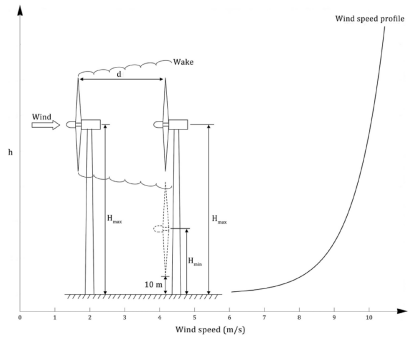

Figure 1: Wind turbines hub height optimization concept to reduce the wake effects [6].

Ahmadreza Vasel-Be-Hagh et al. [6] mention different studies aiming to minimize the wake effect in wind farms by differentiation in turbines' hub height. Lowering the hub height of the next turbine in a line partially reduces the wake streamtube superposition created by a preceding turbine. However, a lower turbine experiences lower wind speeds due to the shear effect of the surface, which reduces the electricity production by this turbine. Figure 1 illustrates the concept of wake losses reduction by hub height optimization [6].

Floating structures, especially semi-submersible platforms, require an extensive amount of materials, such as steel, ballast material, or welds and flanges. The material costs depend on the mass of the platforms, and the unit price of the materials [7]. Reduction of the size of the platforms can significantly reduce the CAPEX, thus reducing the LCOE values for floating offshore platforms [7].

1.1. Objective

The main objective of this work is to investigate the potential LCOE reduction factors in FOW farms. It aims to identify and evaluate techno-economically different strategies that can contribute to the overall performance and profitability improvements of FOW farms. These goals are achieved by aero-hydro-servo-elastic numerical simulations and cost-modeling of different wind farm configurations, varying in turbine spacing distances, turbine hub heights, farm layouts, and the floating platform size.

2. Methodologies and limitations

In this work, a reference wind farm (base case) is defined. It consists of twenty U.S. National Renewable Energy Laboratory (NREL) 5 MW reference horizontal axis wind turbines, described in [8]. The nominal power of the turbines is 5 MW, the rotor diameter is 126 m, the hub height is 90 m above the mean sea level, the rated wind speed is 11.4 m/s and the turbine operates in the wind speed range of 3 m/s to 25 m/s. The turbines are placed on the OC4 semi-submersible platform with structure mass 3.852×10^6 kg, described in [9]. In order to secure the platform, three catenary lines are connected to the platforms and anchored to the seabed. The transmission system of the farm is assumed to comprise an onshore substation (SB), an offshore SB, a high-voltage export cable that connects the onshore SB and the offshore SB, medium-voltage (33kV) array cables, connecting each row of turbines to the offshore SB. The onshore SB is connected to the electrical grid by a high-voltage onshore cable [10].

The turbines are distributed in five rows, each having four wind turbines. The spacing of the turbines is set to 4.3D and the row spacing is 3.3D, with D standing for the turbine rotor diameter.

The wind farm location selected for this study is near the port of Leixões (Atlantic Ocean). The wind farm will be situated at about 35 km distance from the shore and the port. The mean water depth at the location is about 145 m. The characteristic wind-wave climate in the location was estimated based on wind and wave data from the years 1979-2009 reported in [11].

2.1. FAST.Farm

In order to estimate the power generation of the farm and the platform motions, aero-hydro-servo-elastic numerical simulations in NREL's FAST.Farm v3.1.0 software [12] were conducted. FAST.Farm is a midfidelity multiphysics engineering open-source tool developed by NREL, to dynamically simulate power performance and structural loads of turbines through the use of different instances of OpenFAST and other tool modules in a wind farm [12].

FAST.Farm uses a wake dynamics (WD) module, which is based on the the blade element momentum (BEM) theory [13] and the three main dynamic wake meandering (DWM) [14] model principles, namely wake-deficit, wake meandering, and near-wake correction. The wake deficit is modeled by the thin shear-layer approximation of the RANS equations in axi-symmetric coordinates under quasi-steady-state conditions and the turbulence is modeled using the eddy viscosity approach. The wake meandering model is extended to address wake deflection and wake advection in the passive tracer solution. The near-wake correction accounts for wind speed drops and radial expansions of the wake behind the rotor [12]. Additionally, FAST.Farm uses an ambient wind and array effects (AWAE) module, which is used to deter-

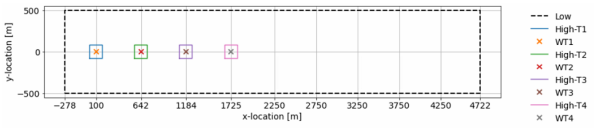

Figure 2: Initial FAST.Farm turbine layout with low and high resolution domains defined. "WT" stands for wind turbine; "Low" stands for the low resolution domain boundary; and High-TX stands for high resolution domain for turbine X.

mine the ambient wind and wake interactions in the wind farm [12]. FAST.Farm uses two domains - a low- and a high-resolution one to simulate different aerodynamic properties. A high-resolution domain is used to simulate the rotor yawing, blade deflection, and the support structure motion along with its loads. The low-resolution domain is needed to save computational power in the wind farm regions that do not require a dense grid and detailed turbulence interpolations [12].

2.2. Simulation settings

The selected simulation time step is set to 0.1 s and the total time to 4200 s. The main output variables chosen are generated power, platform motions, and tower base moments. The size of the LR domain was set to $x = 5000$ m, $y = 1000$ m, $z = 340$ m with the data interpolation step 2.0 s, and nodes spacing 10 m. The size of the HR domains was set to $x = 150$ m, $y = 150$ m, $z = 170$ m with the data interpolation step 0.1 s, and the nodes spacing 5 m. The first turbine is placed 378 m after the start of the domain in the x-direction, as recommended in [12]. LR domain span after the last turbine is equal to around 3000 m in order to allow the wake enough distance downwind of the last turbine for its propagation. The wind turbines' placement for the base case with distances and LR, and HR domains are presented in Figure 2. The hydrodynamics module in the simulations uses a JONSWAP/Pierson-Moskowitz spectrum [15] to create the incident wave time series. All of the wake, and eddy viscosity filter function parameters were set to default FAST.Farm settings, as they were specified for the 5 MW NREL reference turbine, which is used in the simulations. Wind field data was obtained by using TurbSim v2.00.07 software. The timestep of wind interpolation was equal to 0.1 s and the grid size of wind flow was equal to $y = 1000$ m and $z = 340$ m. The spectral wind model used in wind generation is the Kaimal model described in IEC 61400-1 [16]. The turbulence type used was the normal turbulence model, category "B", in accordance with the IEC standard [16]. The wind profile type used was the power law model, with the power law exponent equal to 0.12 [17].

2.3. Evaluation factors' calculation

The generated power results from FAST.Farm were used to calculate the Annual Electricity Production (AEP) for each of the turbines analyzed and consequently, for the whole wind farm. Equation 1 is used to calculate the AEP_{Uw} for each of the wind speed classes.

$$AEP_{\mathrm{Uw}} = \frac{P_{\mathrm{Uw}}\xi_w \cdot 8760}{1000}, \tag{1}$$

where AEP_{Uw} is the annual electricity production for a specific wind speed, represented in MWh, and P_{Uw} is the power generated on the wind turbine for a specific wind speed, represented in kW. The AEP_{Uw} values obtained for the analyzed turbines were summed up for all of the wind speeds, ranging from 3 m/s to 25 m/s and the total annual electricity generated for each turbine AEP_{WT} was obtained. The AEP_{WT} values are represented in GWh.

Afterwards, the total gross wind farm AEP needs to be calculated. Therefore, the AEP_{WT} results for all of the turbines in a row are summed and then multiplied by the number of rows in the wind farm. It is presented in Equation 2,

$$AEP_{\mathrm{farm,\ gross}} = \left(\sum_{i=1}^{4} AEP_{\mathrm{WT}}\right) n_{\mathrm{\ rows}}, \tag{2}$$

where $AEP_{\mathrm{farm,\ gross}}$ is the gross annual electricity production of the wind farm, represented in GWh and $n_{\mathrm{\ rows}}$ is the number of turbine rows in the farm. The net wind farm production $AEP_{\mathrm{farm,\ net}}$ is calculated by including the turbines annual availability, transmission system losses, and airfoil damage losses.

In order to obtain the energy losses due to wakes, the annual electricity production of the simulated farm needs to be compared with an ideal farm operating without the wake losses. As the first turbine in a row is not affected by the wake in the simulations, it is assumed that for the ideal farm, each of the turbines is generating the same amount of electricity as the unaffected turbine.

The capacity factor of the farm is calculated as a percentage, by taking the AEP of the wind farm and dividing it by the theoretical maximal energy yield from each farm. It shows how well the wind farm utilizes the available wind resources. It is represented by

$$CF = \frac{1000 \cdot AEP_{\mathrm{farm,net}}}{P_{\mathrm{T}} n_{\mathrm{T}} \cdot 8760} \cdot 100\% \tag{3}$$

where CF is the farm capacity factor; 8760 is the number of hours in a year and division by 1000 is used for units consistency.

A bigger area of the farm may increase the costs associated with maintenance,and licensing costs, for example. For this reason, an energy yield density factor is defined here as the total annual electricity generated on the wind farm in relation to its area. It is calculated as

$$EYD = \frac{AEP_{\text{farm,net}}}{A_{\text{OWF}}}, \tag{4}$$

where EYD is the energy yield density presented in (GWh/(year· km^2)) and A_{OWF} is the total wind farm area in km^2.

2.4. LCOE calculation methodology

In this study, an economic model evaluating the FOW farm was prepared, based on the literature. As the manufacturers of wind farm components and firms specializing in offshore wind installation do not publicly provide the prices of their products and services, the costs calculations represent only an approximation of the real wind farm costs.

The costs of engineering projects are divided into CAPEX, OPEX and DECEX. In the case of FOW, CAPEX mostly include the development, insurance, and contingency costs, the price of the materials and components, as well as the costs of installation of turbines, floating platforms and other main components. The OPEX are mainly variable costs associated with the maintenance, repairs and operation. DECEX expenditures include, for example, the disassembly, material utilization and area clearance [4, 7].

Based on [18], it is estimated that the contingency, project development, and construction insurance costs' shares amount to 5.5%, 1.1%, and 0.7%, respectively, in relation to the total wind farm costs. Semi-submersible platform material costs comprise the structural steel cost, calculated by taking the structural platform mass and multiplying it by the price of manufactured steel [7]. The cabling costs are calculated by multiplying the unit cost of the individual cables by their distances. The offshore SB cost is calculated as a function of the nominal farm power [7]. The onshore SB cost is estimated as half of the offshore substation expenditures [7, 19]. SCADA system cost has been calculated as the function of the turbines' number [19] and the grid connection total expenditures are assumed to be equal to 2 M€ [19]. Mooring lines' cost is calculated by taking the unit mass of the lines, their length, the unit price of the cables, and the total number of mooring lines and multiplying them. Anchoring costs are calculated by taking the unit costs of the anchors and multiplying them by the number of anchors, which is equal to the number of the mooring lines [7].

The only costs associated with the installation of the turbines are port storage, and onshore turbine mounting on the platforms using a port crane that can be calculated with regards to the port storage surface unit cost, dimensions of the stored turbines, and port crane hourly costs [7].

Therefore, the costs associated with the platforms' installation consist only of the port procedure costs, which require the port crane to launch the platforms into the ocean, calculated in the same manner as the turbine port crane mounting; and the transportation costs which are calculated with regard to the daily rate of tugboats and the time needed to transport all of the platforms [7, 19].

Offshore cables installation is done by cable laying vessels (CLV). The total costs of cable laying depend on the daily rate of CLVs, the length of the cables, and the cable installation speed of the CLVs for specific cable types. The offshore substation is assumed to be floating, so its installation requires the usage of tugboats. Therefore, the costs associated with it consist of the daily rate of the tugboat multiplied by the total installation time, and additionally, of the offshore substation components port storage [19].

Installation of the mooring and anchoring system is done with the help of an anchor handling vehicle (AHV). Therefore, its costs are based on the daily rate of the AHV and the total installation time needed [19]. All of the installation costs that required the usage of different vessels were multiplied by a selected weather-dependent downtime factor, that simulates the inability of offshore installation actions due to bad weather conditions [19].

The values obtained during the OPEX analysis consist of the annual operating and maintenance costs. The operating expenses include onshore wind farm management, marine operations management, weather monitoring, condition monitoring, operating facilities costs; health, safety ad environment (HSE) monitoring, farm insurance, and landlease. The above mentioned values can be calculated according to [19]. OPEX related to maintenance and repair consist of the manual turbine controller reboot cost, minor turbine repair, medium turbine repair, major turbine repair, major replacement, minor foundation repair, minor substation repair, major substation repair, and cable repair. Factors affecting the maintenance costs are the repair time, failure occurrence rate, number of technicians needed, or the vessel used [19]. Similarly to the installation CAPEX calculation methodology, the weather-dependent downtime factor was used in the vessel transportation and repair time calculations [19].

The DECEX were calculated with assumptions that the dismantling costs of the platforms, the cables, the substations, and the mooring and anchoring system are equal to 70%, 10%, 90%, and 90%

of their total installation costs respectively [7].

The LCOE can be calculated as [7]

$$LCOE = \frac{\sum_{i=1}^{T}(CAPEX_i + OPEX_i + DECEX_i)\cdot(1+r)^{-i}}{\sum_{i=1}^{T} AEP_i \cdot (1+r)^{-i}}, \quad (5)$$

where: AEP_i is the annual electricity production in year i; r, the discount rate; T, the lifetime of the project.

2.5. Case studies in this work

The base case is used to define other case studies. In this work, 25 different cases were studied and grouped into four sets. Each case study comprises power generation simulation in FAST.Farm, cost modeling, and calculation of the evaluation factors presented before. Simulations for each studied case were done for 23 different wind speeds (from the turbine cut-in 3 m/s to the turbine cut-out 25 m/s wind speed), resulting in more than 575 simulations performed in this thesis. Due to computational and time limitations, only one row of the farms' is simulated.

The first set of cases was done with the objective of studying the farm performance with respect to different turbine spacings in a wind farm row. The spacings selected were equal to 3D, 4.3D (base case), 6D, 8D, 10D, 12D, 14D, 16D, and 18D, with D being the rotor diameter.

The second set of simulations had the same wind farm layout as the base case, with the objective of turbine hub heights' differentiation. Wind farms having all of the turbines (ALLTRB) hub heights at 78 m, 90 m (base case), 102 m and 109 m were simulated. Additionally, five more cases with different configurations of the turbines hub heights were simulated. The first configuration (90m_78m) has the first and the third turbines' hub height at 90 m, and the second and fourth turbines' hubs at 78 m height. The same arrangement applies to the 102m_78m, 109m_78m, and 109m_90m cases. The 102_78m_seq1221 case has a different hub height sequence, having the first and fourth turbines' hub at 102 m height and the remaining ones at 78 m. When considering different turbine heights, the difference in tower mass is estimated. The mass difference is multiplied by the cost of steel and either added or subtracted from the initial turbines' expenditures in the cost model.

The third set of cases considered different layouts of the wind farm. Two layouts: a diamond-shaped with 2R dephasing, and a dephased-shaped with different dephasing values (1R, 2R, 3R, and 4R) measured in rotor radius R multiples were considered. The diamond-2R layout is presented in Figure 3 (Upper) and a dephased layout with 2R dephasing is presented in Figure 3 (Lower). The diagrams

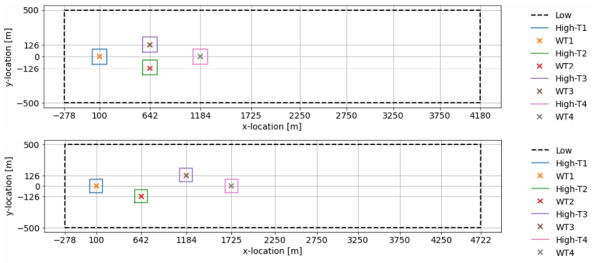

Figure 3: a) Diamond-2R wind farm layout case diagram (Upper), and b) Dephased-2R wind farm layout case diagram (Lower). "WT" stands for wind turbine; "Low" stands for the low resolution domain boundary; and High-TX stands for high resolution domain for turbine X.

present only one row of the farm, as they are simulated in the FAST.Farm software.

The last set of simulations was based on the dephased layout with 2R dephasing and considered different turbine spacings (4.3D, 6D, 8D, and 10D).

Finally, the platform size reduction impact on the LCOE is estimated by a cost-modeling approach, based on an already simulated case with low turbine hub heights.

3. Results and discussion

The simulated power generation of each turbine in the base case was taken to determine the power curves for all of the turbines, shown in Figure 4. WT1 power curve along with the rotational speed and blade pitch angle curves were compared with the NREL 5 MW turbine values [8]. Obtained results are coherent with the NREL values. On the graph, one can notice the differences in power curves for different turbines, with WT1 having generated the highest power up to about 15 m/s, and WT2, WT3, and WT4 operating with lower power output generating 21.8%, 25.9%, and 27.2% less electricity per year, respectively, in comparison to the first wind turbine in a row.

The power curves presented in Figure 4 were used to calculate the evaluation factors for the whole farm. A summary of the results for the base case is presented in Table 1. It is noticeable that the subsequent turbines generate less electricity per year with the highest difference between the first and the second turbine. The wake losses percentage is equal to $\Delta AEP_{\text{wake}} = 18.7\%$ and the capacity factor of the farm is 34.6%.

3.1. Base case cost analysis

The sum of all of the costs needed for the construction, exploitation, and dismantling of the base case wind farm are 712.30 M€. The total capital expenditures for the development phase and materials needed amounted to 440.92 M€, of which the

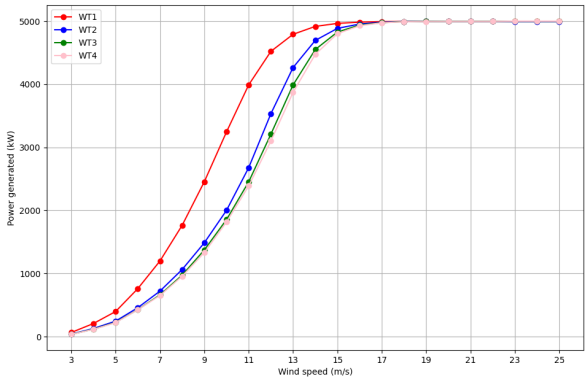

Figure 4: Base case wind turbine power curves.

Table 1: electricity generation, and evaluation factors for the base case.

Name	Value	Unit
AEP_{WT1}	20.6	GWh/year
AEP_{WT2}	16.1	GWh/year
AEP_{WT3}	15.3	GWh/year
AEP_{WT4}	15.0	GWh/year
$AEP_{\mathrm{farm,\ net}}$	302.9	GWh/year
$\Delta AEP_{\mathrm{wake}}$	18.7	%
CF	34.6	%
EYD	112.0	GWh/(year $\cdot$ km^2)

largest costs are for the SS platforms. Total installation costs associated with the construction of the wind farm were 43.29 M€. The OPEX amount to 223.31 M€ (95.35 M€ when discounted) during the project lifetime. It was found that the annual OPEX reached a value equal to 8.93 M€/year, of which wind farm operational expenditures were 3.17M€, and the maintenance costs were 5.76 M€. The DECEX amounted to 14.76 M€. To evaluate the LCOE, a discount rate, determined for developed countries, equal to WACC = 8% [20] was chosen. The LCOE for the total lifespan of the base case farm (25 years) is **168.85 EUR/MWh**. Obtained LCOE value for the base case wind farm is in line with the values published in [18].

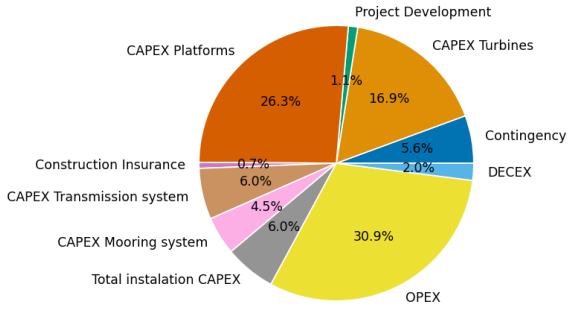

Figure 5: Base case total wind farm expenditures percentage shares estimated based upon the cost model in this thesis.

Based on the cost analysis, a pie chart, presented in Figure 5 was created, that shows the share of individual expenses in relation to the total costs of the project. The chart shows that the largest contribution to the total expenses for the wind farm makes the CAPEX, which together amount to as much as 67.1%. The OPEX expenses are equal to 30.9% and the DECEX cover 2% of the total expenses. The obtained expenses shares were compared to a study done by NREL [18]. It can be noticed that the shares of different cost components obtained in this study are similar to the ones listed in the reference paper, especially the turbines and platforms expenses, installation and commissioning costs, OPEX and DECEX values. The transmission system values are undervalued in comparison to the NREL report. However, these expenses are deeply based on the cable lengths and the farm distance from the shore and are dependent on the specific farm designs.

3.2. Turbine spacing variations

The obtained values of the evaluation factors for the turbine spacing cases set are presented in Figure 6. The AEP values in Table 2 present an increasing trend with the turbine spacing. The annual net electricity production of the farms is presented in Table 2.

Table 2: Net annual electricity farm production for different turbine spacing variations.

Turbine spacing	$AEP_{\mathrm{net,\ farm}}$ $(\frac{\mathrm{GWh}}{\mathrm{year}})$
3D	281.4
Base case - 4.3D	302.9
6D	322.2
8D	336.7
10D	346.1
12D	391.9
14D	397.8
16D	402.2
18D	406.2

As one can notice from Figure 6, increasing the distance between consecutive turbines from the Base Case 4.3D to 18D can reduce the wake losses from 18.7% to 1.5%. The decrease tends to be non-linear, therefore, further turbine spacing increase would result in lower differences in wake losses reaching a point, where the losses decrease would be negligible. The LCOE values also tend to decrease with the turbine spacing distance, however, the decline is also non-linear, due to the non-linear decline of the wake losses explained above and increasing costs of components (e.g. array cables and maintenance expenditures). Because of that, the LCOE values reach a point, where the wake losses differences become negligible, compared to the costs, and lead to a point, from which the continuously in-

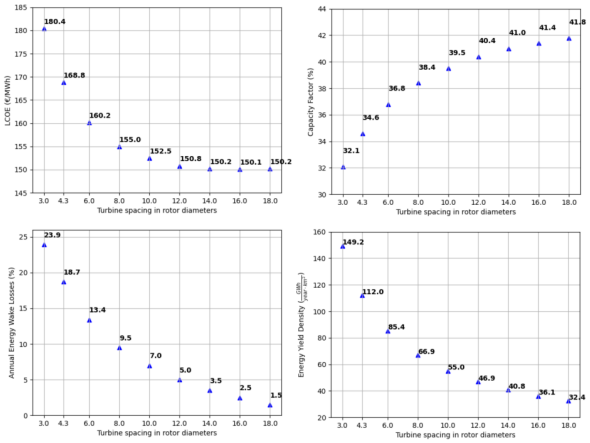

Figure 6: Evaluation factors for different wind turbine spacings.

creasing expenditures will surpass the AEP gains from wake losses reduction. Analyzing the results in this study, this phenomenon occurs at the 14D to 16D spacing range, from where the LCOE values start to rise. Based on that and relatively low differences between capacity factors at this range, the most energy- and cost-efficient turbine spacing may lie within the 12D to 14D span, where the levelized cost of energy values can be decreased by 10.7% and 11.0%, respectively, compared to the base case. However, this must be considered a qualitative observation, due to uncertainties associated with the assumed LCOE and energy calculations.

On the other hand, the energy yield values show a significant decrease with the spacing distance at lower spacing (3D - 10D), and a smoother decrease in the larger spacing. A larger wind farm area takes up more, which makes it more difficult for maritime vehicles to navigate through. It can also lead to longer installation and maintenance work times, which need to be addressed, but are difficult to quantitatively determine, due to a lack of commercially available information.

3.3. Turbine hub height variations

In order to estimate the impact of higher hub heights on the platform movements, an analysis of minimum and maximum platform motion values was done in FAST.Farm. The examined results are presented in Figure 7. According to the performed simulations, the platform maintained its stability for every hub height case. The biggest relative difference can be observed in the roll and yaw motion. When it comes to the surge motion, the differences are negligible. In regards to the mooring lines' loads, the platform movements were compared with the mooring load-displacement analysis performed by NREL in [9]. None of the mooring lines' loads, exerted by the platform movements, surpassed the failure values.

In order to check the impact of the turbine heights on the moments exerted on the base of the turbine towers, maximum x-, y- and z-direction tower base moments were simulated using the FAST.Farm software. The highest obtained maximum moment values were exerted on the tower base in the y-direction, thus they are presented in Figure 8. It can be noticed that the 102 m and 109 m turbine hub height towers' y-direction base load moments are significantly higher compared to the base case. Increased tower base moments escalate the fatigue on the turbine towers, which may lead to a decreased lifetime of the farm, or increased maintenance expenditures due to a higher probability of turbine malfunction.

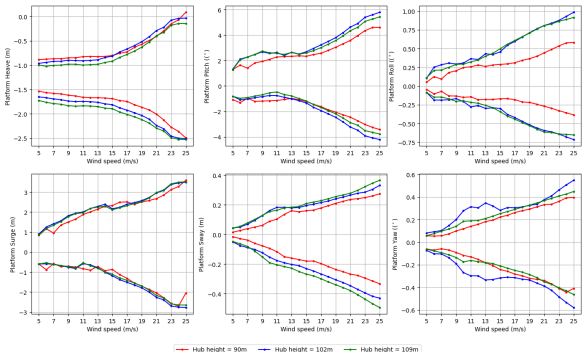

Figure 7: Maximum and minimum platform movements for turbines with the 90 m, 102 m, and 109 m hub heights.

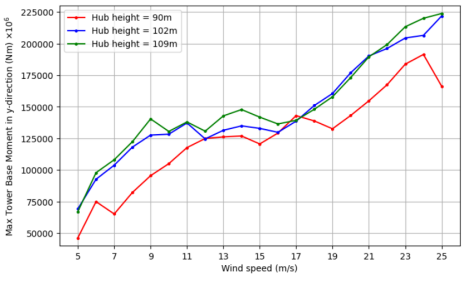

Figure 8: Maximum moments on the base of the turbine tower in the y-direction for turbines with 90 m, 102 m, and 109 m hub heights.

The net AEP results for all of the cases are presented in Table 3. Looking at the results, it can be noticed, that the highest and the lowest AEP were obtained for the ALLTRB_109m and ALLTRB_78m cases, respectively. Differentiation in consecutive turbine hub heights has shown lower annual electricity production values compared to their reference ALLTRB cases. The 90m_78m, 102m_78m, 109m_78m, and 109m_90m cases

had obtained lower AEP values than the ALLTRB_90m, ALLTRB_102m, and ALLTRB_109m respective cases. It means, that the energy wake losses reduction due to the differentiation in consecutive turbine hub heights is lower than the energy yield increase due to the higher hub heights. The 109m_90m and the 109m_78m configuration have both obtained the same annual electricity production. The 109m_78m variation has obtained lower wake losses than the 109m_90m configuration. However, the energy losses due to the wake effects are compensated by higher wind speeds at elevations of 90 m compared to 78 m, which result in higher power generation of the 90 m turbines in the 109m_90m variation compared to the other configuration, and this may be the cause of equal AEP values.

Having smaller turbine towers lowers the CAPEX of the wind farm, which is why the LCOE values need to be taken into consideration as well. The LCOE, along with other evaluation factors are presented in Figure 9.

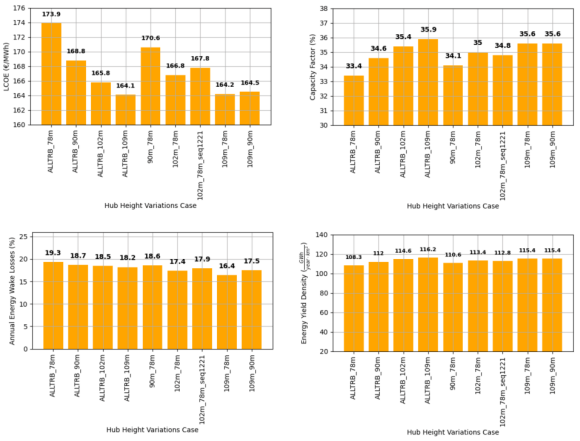

Figure 9: Evaluation factors for different wind turbine hub height variations.

Table 3: Net annual electricity farm production for different turbine hub height variations.

Turbine hub height variation	$AEP_{\textbf{net, farm}}$ $(\frac{\textbf{GWh}}{\textbf{year}})$
ALLTRB_78m	292.8
Base case ALLTRB_90m	302.9
ALLTRB_102m	309.9
ALLTRB_109m	314.1
90m_78m	299.1
102m_78m	306.7
102m_78m_seq1221	304.8
109m_78m	312.1
109m_90m	312.1

As one can notice, looking at the graph 9, the lowest LCOE values were obtained for the ALLTRB_109m case, followed by the 109m_78m, 109m_90m, and ALLTRB_102m cases. The lowest energy wake losses were obtained for the highest differences in consecutive turbine hub height configurations (109m_78m, 102m_78m, and 109m_90m), which means that the wake losses reduction can be obtained by varying the turbine hub heights in the farm. Nevertheless, this reduction of the wake losses is too small to make a significant power generation difference in the simulated cases. Additionally, the turbine material CAPEX savings are too low to compensate for the decreased energy yield of the lowered turbines.

Considering the results and the aforementioned higher fatigue issues, varying turbine hub heights may not provide a profitable and viable solution for wake losses and LCOE reductions. However, the cost model considers only the material cost, and not manufacturing and labor expenditures reductions, which may contribute to a levelized cost of energy reduction.

3.4. Wind farm layout variations

The AEP results for different wind farm layouts are presented in Table 4. Clear differences in $AEP_{\text{net, farm}}$ compared to the base case can be seen. As the dephasing radius increases, the value of annual electricity production increases. For the analyzed 4R-dephasing case, a 21% higher value was observed with respect to the base case. The dephased-2R layout demonstrated a slightly higher annual electricity production values $AEP_{\text{net, farm}} = 353.4$ (GWh/year) compared to the diamond-2R layout with $AEP_{\text{net, farm}} = 349.5$ (GWh/year). The analysis of the data obtained from the simulations performed showed that the highest AEP value was obtained for the dephased_4R wind turbine configuration.

Table 4: Net annual electricity farm production for different wind farm layout variations.

Turbine hub height variation	$AEP_{\textbf{net, farm}}$ $(\frac{\textbf{GWh}}{\textbf{year}})$
Base case - 4.3D	302.9
4.3D_Dephased_1R	331.1
4.3D_Dephased_2R	353.4
4.3D_Dephased_3R	363.3
4.3D_Dephased_4R	366.4
4.3D_Diamond_2R	349.5

The graphs showing the evaluation factors' values are presented in Figure 10. As one can notice from Figure 10, both layouts show a significant decrease of LCOE values compared to the base case, with 13.3% and 14.3% decrease for the diamond-2R and dephased-2R layout respectively. Energy wake losses were also significantly decreased to 6.1% and 5.1% for the diamond-2R and dephased-2R layouts, which correspond to the wake losses decrease of 10D - 12D turbine spacing. The differences in LCOE, ΔAEP_{wake}, and capacity factors between both of the layouts are small. However, the energy yield density results showed a substantially higher value

for the diamond layout compared to the dephased one. Based on the small differences in LCOE, CF, and wake losses between the two cases, and significantly higher EYD values in the diamond layout, it can be stated that the diamond layout is better and could be further researched.

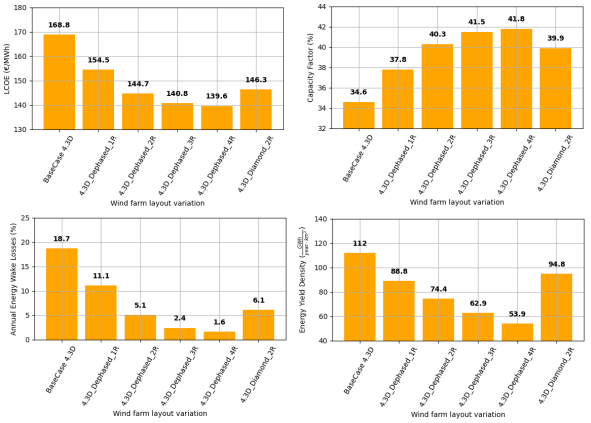

Figure 10: Evaluation factors for the diamond-shape and dephased-shape wind farm layouts.

When analyzing the results of different R-dephasing values, presented in Figure 10, it can be noticed, that dephasing the turbines significantly reduces the wake losses, even down to 1.6% for the 4R-dephasing compared to the base case with losses of 18.7%. The wake losses present a similar, non-linear trend to the turbine spacing simulation cases set, with negligible wake losses differences between the 3R- and 4R-dephasing. Therefore, the LCOE trend is non-linear and similar to the one obtained in the first case study set. That is why, it is expected that the wake losses reduction will become so small, that the increasing expenditures caused by larger farm areas will surpass the AEP gains from further turbine dephasing leading to an inflection point. As the LCOE, wake losses, and capacity factor differences between the 3R and the 4R case are negligible and the energy yield differences are significant, it can be stated that the highest profitable dephasing distance is 3R.

3.5. Dephased layout turbine spacing variations

When analyzing different turbine spacing variations in the dephased-2R layout, it can be noticed, that longer distances between the turbines in a row show small differences between the analyzed configurations, indicating the negligible impact of the distribution of turbines in rows on the performance of dephased wind farms. The AEP for the 10D spacing, equal to 361.8 GWh/year is only 2.3% higher compared to the 4.3D spacing in the dephased-2R layout. The LCOE results, due to the larger farm areas and therefore, higher expenditures, showed a decreasing trend with the increasing turbine spacing in the 2R-dephased case. The LCOE for the 10D spacing is 145.9 GWh/year, which is 0.8% higher than the LCOE for the 4.3D spacing. The energy wake losses and CF differences between different cases are very low as well. The largest differences were registered in the case of the EYD analysis, with a decreasing trend observed. The EYD for the 10D spacing is 32.7 GWh/(year$\times$km^2), which is 60% lower than the 4.3D EYD equal to 74.4 GWh/(year$\times$km^2). Based on the above, the impact of increased turbine spacing in this case is negative, although insignificant, and the most cost-efficient configuration analyzed in this simulation set is the 4.3D_Dephased_2R one.

3.6. Floating platform size variations

Before attempting to simulate additional cases with the floating platform size variations, a quick estimation of the LCOE values was done, based on the ALLTRB_78m case. Different platform size reductions, ranging from 2% to 10% with a 2% step, were applied to the cost model used in this thesis. The variable affected by the scaling was the platform structural mass. Based on the analysis, it can be noticed, that the platform size reduction has a low impact on the levelized cost of energy, lowering the LCOE by 3.4% at a 10% platform size reduction. Considering the low impact of platform size reductions on the LCOE and uncertainty over platforms' destabilization, the simulations of the platform size variations were not done in this thesis.

4. Conclusions

Different strategies for the cost of energy reduction in floating wind farms were explored techno-economically. More than 575 simulations were performed using FAST.Farm, based on various sets of cases. The first set of cases involved different turbine spacing variations analysis. Results showed that the most profitable solutions were obtained for spacings of 12D and 14D. It can be noticed that the LCOE values reach a point, where the wake losses differences between subsequent spacings become negligible, and compared to the costs, lead to a LCOE function change, from which the continuously increasing expenditures surpass the AEP gains from wake losses reduction.

Another set of cases involved the wake loss reduction analysis by varying the turbine hub heights in the farm. The reduction of the wake losses is too small to make a significant power generation difference in the simulated cases. Additionally, the turbine material CAPEX savings are too low to compensate for the decreased energy yield of the lowered turbines, leading to small LCOE differences between the cases.

The wind farm layout set of cases' results showed improvements regarding the AEP and LCOE. The

energy wake losses were significantly decreased down to 6.1% and 5.1% for the diamond and dephased layouts. The energy yield density results showed a substantially higher value for the diamond layout compared to the dephased one. Based on that, it may be stated that the diamond wind farm layout is better compared to the other studied layouts. Further analysis, that simulates the wake effects of a complete farm to determine the most cost-efficient distance between the turbine rows is recommended.

Increasing the dephasing distance, reduces the wake losses, even down to 1.6% for the dephasing equal to 4R. A significant reduction in the LCOE of 16% and 17.2% for the 3R and 4R dephasing, respectively. Therefore, it is recommended to look into different wind farm layouts. The turbine spacing does not significantly influence the performance and LCOE of wind farm's, when considering the dephased wind farm layouts.

Based on an estimation done in regards to the platform size reduction, down-scaling of the floating platform may not have a high impact on the LCOE. The estimation done, using the cost model in this thesis, shows a 3.4% of LCOE decrease for a 10% platform size reduction. Furthermore, such a reduction of the platform size may significantly impact the platform dynamics and may lead to platforms' destabilization, especially when considering higher turbine hub heights and greater weight.

References

[1] W. Lamb et. al. A review of trends and drivers of greenhouse gas emissions by sector from 1990 to 2018. *Environmental Research Letters*, 16, 07 2021.

[2] IRENA. Future of wind: Deployment, investment, technology, grid integration and socio-economic aspects (a global energy transformation paper), 2019.

[3] V. N. Dinh and E. McKeogh. Offshore wind energy: Technology opportunities and challenges. In M. F. Randolph, D. H. Doan, A. M. Tang, M. Bui, and V. N. Dinh, editors, *Proceedings of the 1st Vietnam Symposium on Advances in Offshore Engineering*, pages 3–22, Singapore, 2019. Springer Singapore.

[4] A. Martinez and G. Iglesias. Multi-parameter analysis and mapping of the levelised cost of energy from floating offshore wind in the mediterranean sea. *Energy Conversion and Management*, 243:114–416, 2021.

[5] Al-Addous et. al. The significance of wind turbines layout optimization on the predicted farm energy yield. *Atmosphere*, 11(1), 2020.

[6] A. Vasel-Be-Hagh and C. L. Archer. Wind farm hub height optimization. *Applied Energy*, 195:905–921, 2017.

[7] C. Maienza et. al. A life cycle cost model for floating offshore wind farms. *Applied Energy*, 266:114716, 2020.

[8] J. Jonkman et. al. *Definition of a 5-MW Reference Wind Turbine for Offshore System Development. NREL/TP-500-38060.* NREL, February 2009.

[9] A. Robertson et. al. *Definition of the Semisubmersible Floating System for Phase II of OC4. NREL/TP-5000-60601.* NREL, September 2014.

[10] M. Rentschler et. al. Parametric study of dynamic inter-array cable systems for floating offshore wind turbines. *Marine Systems & Ocean Technology*, 15, 01 2020.

[11] J. C. C. Portillo. *Oscillating-water-columns systems: single devices, arrays, and multipurpose platforms.* PhD thesis, Instituto Superior Técnico, University of Lisbon, 2022.

[12] J. Jonkman and K. Shaler. FAST.Farm user's guide and theory manual, 2021. url: https://www.nrel.gov/docs/fy21osti/78485.pdf. Accessed: 31-10-2022.

[13] S. A. Ning. A simple solution method for the blade element momentum equations with guaranteed convergence. *Wind Energy*, 17(9):1327–1345, 2014.

[14] G. C. Larsen et. al. *Dynamic wake meandering modeling.* Number 1607(EN) in Denmark. Forskningscenter Risoe. Risoe-R. Risø National Laboratory, 2007.

[15] W. J. Pierson Jr. and L. Moskowitz. A proposed spectral form for fully developed wind seas based on the similarity theory of s. a. kitaigorodskii. *Journal of Geophysical Research (1896-1977)*, 69(24):5181–5190, 1964.

[16] IEC 61400-1. Wind turbine generator systems-part 1: Safety requirements, 1999. 2nd edition, Geneva, Switzerland.

[17] M. Argin et. al. Exploring the offshore wind energy potential of turkey based on multi-criteria site selection. *Energy Strategy Reviews*, 23:33–46, 2019.

[18] T. Stehly and P. Duffy. 2020 cost of wind energy review, 2021. url: https://www.nrel.gov/docs/fy22osti/81209.pdf, Accessed: 31-10-2022.

[19] J. Lappalainen. Economic potential of offshore wind energy in the Gulf of Bothnia. Master's thesis, Aalto University. School of Electrical Engineering, 2019.

[20] L. Cozzi et. al. Offshore wind outlook 2019. Technical report, IEA, 2019.